Research

iMedPub Journals
www.imedpub.com

Nano Research & Applications
ISSN 2471-9838

2022
Vol.8 No.12:102

Optimized Green Synthesis of Magnetite-Gold Composite Nanoplatform by Aqueous Extract of *Malva Sylvestris* Leaf as a Photothermal Therapy Agent

Monika Joharian[1], Mahdi Mojarab[1], Viana Nazari[1], Behrang Shiri Varnamkhasti[1*] and Somayeh Mirsadeghi[2*]

[1]Department of Pharmacy, Kermanshah University of Medical Sciences, Pharmaceutical Sciences Research Center, Kermanshah, Iran

[2]Department of Science and Technology, Sharif University of Technology, Science and Technology Park, Tehran, Iran

[*]**Corresponding author 1:** Behrang Shiri Varnamkhasti, Department of Pharmacy, Kermanshah University of Medical Sciences, Pharmaceutical Sciences Research Center, Kermanshah, Iran, E-mail: shiribehrang@yahoo.com

[*]**Corresponding author 2:** Somayeh Mirsadeghi, Department of Science and Technology, Sharif University of Technology, Science and Technology Park, Tehran, Iran, E-mail: sshmirsadeghi@sina.tums.ac.ir

Received date: November 15, 2022, Manuscript No. Ipnto-22-15034; **Editor assigned date**: November 17, 2022, PreQC No. Ipnto-22-15034 (PQ); **Reviewed date**: November 28, 2022, QC No. Ipnto-22-15034; **Revised date**: December 07, 2022, Manuscript No. Ipnto-22-15034 (R); **Published date**: December 15, 2022, DOI: 10.36648/2471-9838.8.12.102

Citation: Joharian M, Mojarab M, Nazari V, Varnamkhasti BS, Mirsadeghi S (2022) Optimized Green Synthesis of Magnetite-Gold Composite Nanoplatform by Aqueous Extract of *Malva Sylvestris* Leaf as a Photothermal Therapy Agent. Nano Res Appl Vol. 8 No.12:102

Abstract

Photothermal therapy is a non-invasive method for early detection and treatment of cancers that uses nanostructures or nanomaterials as the agent of photothermal therapy, and these nanostructures emit heat by absorbing near infrared light, which due to *in situ* application; it does the least damage to normal cells. In the present research, magnetite-gold composite nanoplatform (Fe_3O_4/Au) in the size range of 30-45nm were successfully synthesized using a fast, non-hazardous, cost-effective and biocompatibility biosynthetic procedure by reduction of ferric chloride and gold solutions with the aqueous natural extract of a plant namely *Malva sylvestris* as an original factor which acts as reducing agent and efficient stabilizer without addition of any chemical reducing agents or surfactants for the first time. Fe_3O_4-Au-nanocomposite characteristics were studied by using FT-IR, XRD, FE-SEM, EDX, DLS, Zeta sizer and UV–Vis techniques. The impacts of some synthesis agents like cation concentrate, the amount of plant leaf, mass of Fe_3O_4 and Au salt and temperature of extraction were investigated and optimized to achieve the best size of Fe_3O_4/Au nanocomposite. The results showed that the synthesis of Fe_3O_4/Au-nanocomposite was economically cheap when compared with usual methods. Furthermore, the nanocomposite synthesized through this biosynthesis, green method can potentially useful in different applications, and green nanotechnology fields as an excellent option, such as tumor photothermal therapy method for cancer.

Keywords: Fe_3O_4/Au nanocomposite; Plant extract; Green synthesis; Cancer; Photothermal therapy

Introduction

Cancer is a continuing tension for general health around the world because of its fatality and incursion. Nowadays, some commonly used strategies, such as chemotherapy, radiotherapy, are still used for cancer treatment even though they are usually accompanied by wide side injury [1,2]. Accordingly, researches on invasive and selective therapies have been important issues in the antitumor therapy. One of the most important and selective treatments s in the recently years that has received wide attention is light stimulation therapy, such as Photo-Thermal Therapy (PTT) [3,4]. Thermal treatments versus cancer depend on the sensitivity of cancer cells to heat and they have a less ability to tolerate increased heat [5]. In fact, heat makes irreparable harm to cancer cell membranes [6-12]. To produce heat, the light irradiation employed should be able to pass *via* healthy tissues without creating any side effect. Different from ultraviolet light and visible light, near infrared light can infiltrate deep tissues and it deals relatively moderate damage [13-15]. So far, various nanostructured materials that have intense NIR absorbance have been applied as photothermal and ablation factors for extinguishing cancer cells, such as Au-based structures, carbon-based nanomaterials, platinum NPs, CuS nanoparticles, and the conducting polymers [16-20]. As well as, nanostructured materials are able to cross through cancer cell membranes leading to increasing treatment efficacy. In recent years, researchers have paid much attention to the use of gold nanoparticles among other nanomaterials for Photo-Thermal Therapy (PTT). Au NPs without any change have an SPR effect in the area of visible light [21]. Various gold nanomaterials have been used to tune the SPR and increase the photothermal performance, for instance Au nanorods, gold nanoshells and so on [22,23]. It was introduced that the gold nanoparticles could be coated with other nanomaterials such as Fe_3O_4 magnetic NPs to improve thermal performance [24]. Recently, the enhancement in the application of nanoparticles has led to expand green synthetic methods. In these researches and investigations, the use of procedures and reagents that generate toxic manufactured nanoparticles are avoided in order to create environmentally friendly processes. One of the most common techniques is the use of plant extracts to green synthesize NPs.

© Copyright iMedPub | This article is available from: https://nanotechnology.imedpub.com/archive.php

This method is simple, eco-friendly, low cost and safe for human therapeutic application. Further, it is a single step method and it is appropriate for large-scale production. Accordingly, these features have caused this route as a better option than traditional synthetic procedures particularly for photothermal therapy.

In this project, for the first time, the extract of a native plant of Iran, called malwa, will be used as a green and safe reagent for the synthesis of magnetite-gold nanocomposite, and there is no need to purchase substances that reduce and stabilize nanoparticles. Among the many plants that are used in traditional medicine, *malva* stands out due to its diverse applications. *Malva* belongs to the Equistopsida category, the family of *Khatami* and *malva* species, which has many benefits and properties, such as: anti-inflammatory, anti-wound, antiseptic, anti-diarrheal and treatment of respiratory problems. It also has phytochemical elements including: Amino acids/ protein derivatives, flavonoids, terponoids, enzymes, vitamins, *etc.* Because of the extensive usage and medicinal significance of *malva*, numerous studies have been done.

Experiment

Materials and measurements

All chemicals used were commercially available from the Merck and Sigma Aldrich Companies. FT-IR spectra were recorded using an IR Prestige-21 spectrophotometer from the Shimadzu Company. X-ray powder diffraction measurements were performed using Xpertpro from Panalytical company with Cu K α radiation (λ=1.5405 A˚). The morphology and chemical composition of samples of the obtained nano materials were evaluated by FE-SEM and EDX using a MIRA3 TESCAN microscope. Particle size distribution was measured by a Dynamic Light Scattering (DLS)-Malvern Zetasizer 2000. The synthesize of nanoparticles was monitored by an UVmini-1240, Shimadzu spectrophotometer. *Malva sylvestris* leaves were prepared from Iranian Plants Center.

Preparation of *Malva sylvestris* leaves extract

First, 5 gm of dried leaves of this plant were poured into an Erlenmeyer flask and made up to 100 ml with distilled water. The obtained mixture was then boiled on a heater and the resulting extract was cooled by Whattman paper after cooling. Finally, in order to separate the larger particles, the extract was centrifuged at 5000 rpm for 10 min and finally placed in the refrigerator at 4°C to continue working.

Synthesis of Fe_3O_4 NPs

Magnetite nanoparticles were synthesized by a green procedure. At first the $FeCl_2.4H_2O$ and $FeCl_3.H_2O$ solutions (0.1 M) were prepared, next these solutions were blended in a ratio of 2:1 (under N_2 gas injection), and afterward a 10 mL of extract was added to this solution (brown color). The finally solution was stirred for some minutes and in the end, a few drops of NaOH were poured to the solution. The color variation from brown to black shows that the magnetite nanoparticles were synthesized (Figure 1). Eventually, the obtained nanoparticles were collected by magnet, washed three times with distilled water, and dried in an oven at 70°C for 24 hrs.

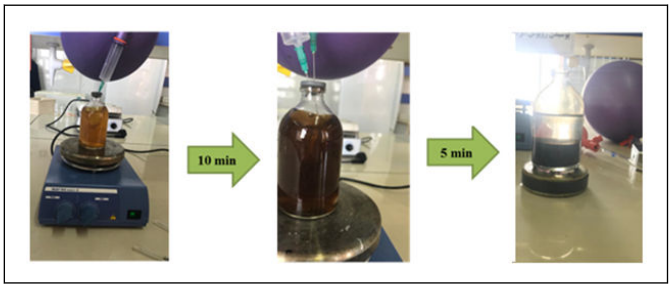


Figure 1: Synthesis of iron oxide nanoparticles.

Synthesis of Fe_3O_4/Au nanocomposite

Initially, magnetite nanoparticles with the extract were placed on the heater and on the other hand, 10 ml of gold salt with the Specific concentrations was placed on the heater to boil. After the temperature of the magnetite nanoparticles as well as the extract reached the above-mentioned temperatures, boiling gold salt was added to it and by stopping the temperature for 5 min, it was sterilized at high speed. The synthesized composite nanoparticles were then collected by magnet and washed three times with distilled water. At last the obtained nanoparticles were dried at ambient temperature and used for other analyzes (Figure 2).

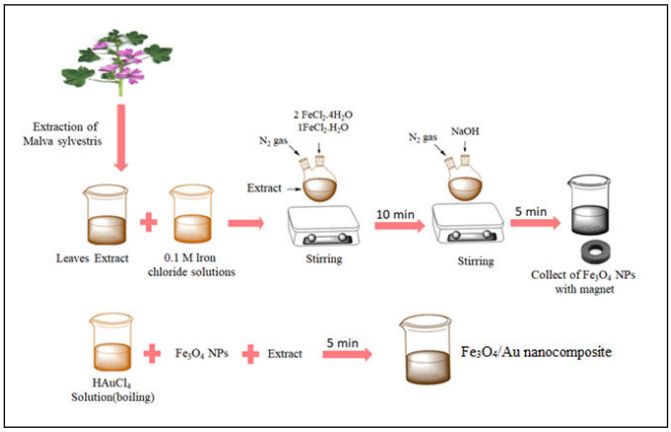


Figure 2: General method for green synthesis of Fe_3O_4/Au nanocomposite.

Different factors (temperature, extract amount, Fe_3O_4 amount and gold salt concentration) for the synthesis of magnetite-gold nanocomposite by a green method were evaluated, which are shown in Table 1. In order to optimize the synthesis of nanocomposite, various parameters including the concentration of magnetite nanoparticles, the amount of *Malva sylvestris* extract, the reaction temperature and the concentration of gold salt were evaluated. The uses of magnetite were 0.5 and 0.1 g, the amount of plant extract was 10 and 25 ml, the reaction temperatures were 30, 45 and 60°C, and the concentrations of gold salt were 1 and 5 mM. After 15 samples were synthesized based on the stated parameters, based on the UV spectrum and based on DLS data (Table 1S), the optimal sample (sample 5),

which also had appropriate values in terms of size, was selected for further experiments.

Trial conditions	Mass of Fe_3O_4 (gr)	Cation concentrate (mM)	Mass of plant (mL)	Temperature (◦c)
1	0.1	1	25	60
2	0.1	5	25	60
3	0.5	1	25	60
4	0.5	5	25	60
5	0.1	1	10	45
6	0.1	5	10	45
7	0.5	1	25	45
8	0.5	5	25	45
9	0.1	1	10	30
10	0.1	5	10	30
11	0.5	1	25	30
12	0.5	5	25	30
13	0.1	1	10	30
14	0.5	1	10	45
15	0.5	1	10	60
*In all samples, the amount of gold salt solution was 10 mL and its temperature was boiling.				

Table 1: Different conditions for the green synthesis of magnetite-gold nanocomposite.

Results and Discussion

Characterization of the Fe_3O_4 NPs and Fe_3O_4/Au nanocomposite by DLS, UV, FT-IR and PXRD analyses

Au/Fe_3O_4 nanocomposite was synthesized by an environmentally friendly method in the presence of *Malva sylvestris* leaves extract. *Malva sylvestris* extract as a reductant of metal ions decreases their agglomeration, arranges the morphology of the NPs, and enhances their stability. A variety of factors (extract amount, temperature, Fe_3O_4 amount and gold salt concentration) were evaluated, which are shown in Table 1.

DLS measurement was used to characterize the size distribution of nanoparticles. In this technique, the hydrodynamic radius of the nanostructured materials and their dispersion index were determined. The results indicated that the prepared nanocomposite had dissimilar Rh and particle size dispersion indices at various temperatures and concentrations (Table 1S). Among the synthesizes Fe_3O_4/Au nanocomposites, sample 5 had smaller hydrodynamic radii and better dispersion index than the others, which shows that nanoparticles with uniform size were synthesize homogeneously (Figures 3 and 4).

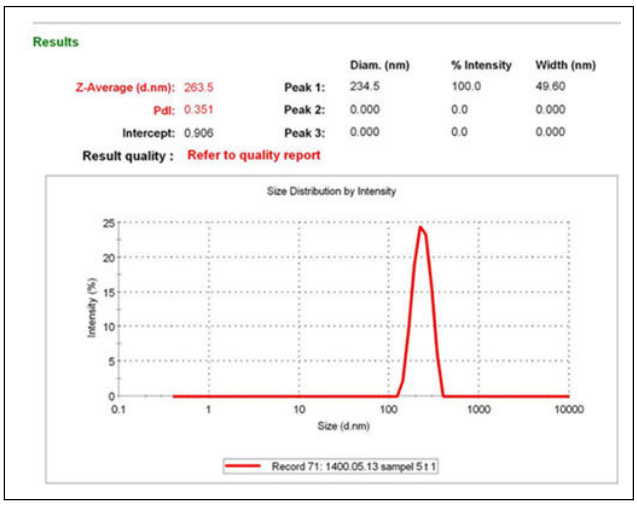


Figure 3: Hydrodynamic radius and dispersion index of sample particle size 5.

© Copyright iMedPub

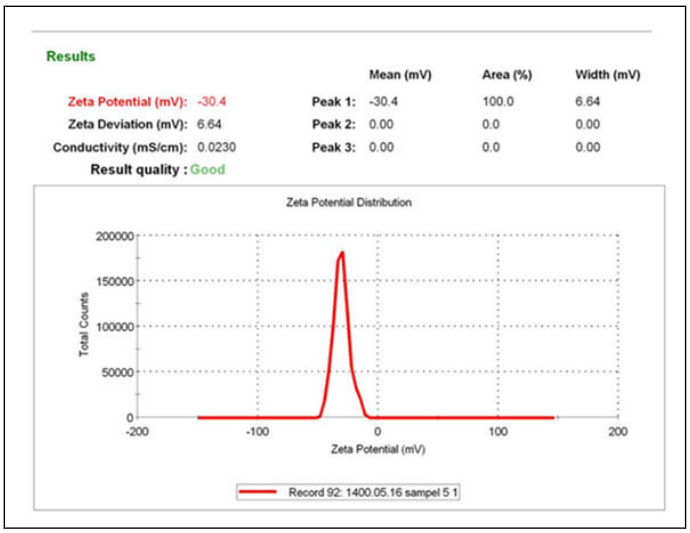


Figure 4: Zeta potential of magnetite-gold composite nanoparticles (sample 5).

According to Table 1S, selective sample 5 was chosen for further measurements and also better dispersion index than the others. One of the important parameters in the stability of nanoparticles is zeta potential or the surface charge of nanoparticles. Zeta potential greater than ± 30 indicates that nanoparticles have high stability and aggregation does not occur in them, or if it does occur, it is less. Therefore, the results displayed that the obtained nanocomposite has a negative charge of 30 mV, which indicates the high stability of the prepared nanocomposite. The synthesized Fe_3O_4 NPs and Fe_3O_4/Au nanocomposite (sample 5) were examined by UV–Vis spectroscopy (200-800 nm) to verify the synthesis of Au/Fe_3O_4 nanocomposite using *Malva sylvestris* leave extract (Figure 5 and Figure 6). In all cases 1ml of sample to conduct the analysis was employed.

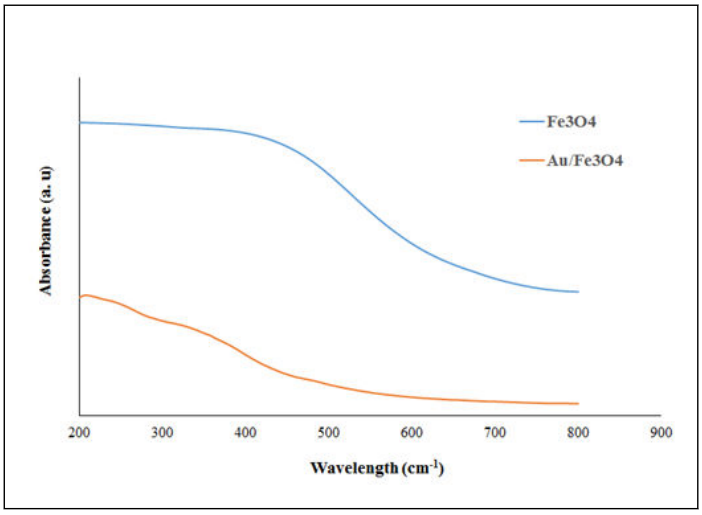


Figure 5: UV spectrum Fe_3O_4 nanoparticles and Fe_3O_4/Au nanocomposite (sample 5).

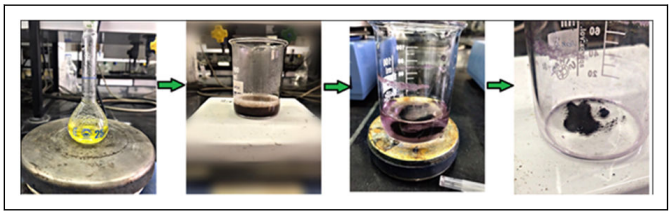


Figure 6: Steps of preparation of magnetite-gold composite nanoparticles.

The XRD patterns of the biosynthesized Fe_3O_4 NPs and Fe_3O_4/Au nanocomposite (Figure 7) indicate eight intense peaks with 2θ values of 30.3°, 35.6°, 43.3°,53.6°, 57.4° and 62.9°, respectively in all the composites which shows the crystalline cubic spinel structure. Moreover, the reflection peak positions and intensities of Fe_3O_4 NPs agree well with the XRD patterns in the literature (JCPDS Card No: 19-629) that displays the nanoparticle structure is well synthesized. The peaks located in the 44.3° and 77.6° are related to gold nanoparticles, furthermore to the peaks of iron oxide nanoparticles, indicates the synthesis of magnetite-gold composite nanoparticles, which has been obtained correctly in sample 5.

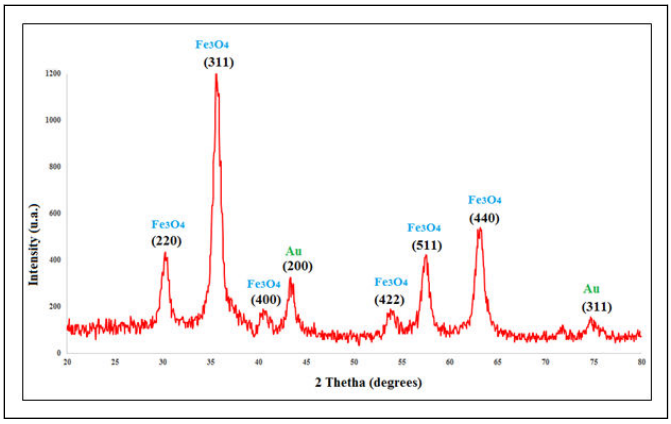


Figure 7: XRD pattern of Au/Fe_3O_4 nanocomposite (sample 5).

The FT-IR spectra (Figure 8) display the absorption bands for Au/Fe_3O_4 nanocomposite. The absorption approximately 580 cm^{-1} in sample 5 (assigned to Fe-O stretching vibrations); 3400 cm^{-1} (O-H stretching vibrations of carboxylic acid from the *Malva sylvestris* extract); 2924 cm^{-1} (C-H stretching); 1618 cm^{-1} (overlapping peaks of alkene (C=C) or (C=O)) and 1000 cm^{-1}-1350 cm^{-1} (C-O phenolic stretching) [25]. In the magnetite-gold nanocomposite spectrum, the same peaks are observed for magnetite nanoparticles, but there are displacements that are related to the addition of gold nanoparticles to the nanoparticle structure. For example, the peak of 1060 cm^{-1} in magnetite nanoparticles has shifted to 1089 cm^{-1} in magnetite-gold nanocomposites. Peaks in the range of 1070 to 1090 cm^{-1} and 1625-1650 cm^{-1} are among the peak peaks of gold nanoparticles [26,27]. On the other hand, the 1610 peak in magnetite nanoparticles that has shifted to 1629 cm^{-1} in nanocomposites.

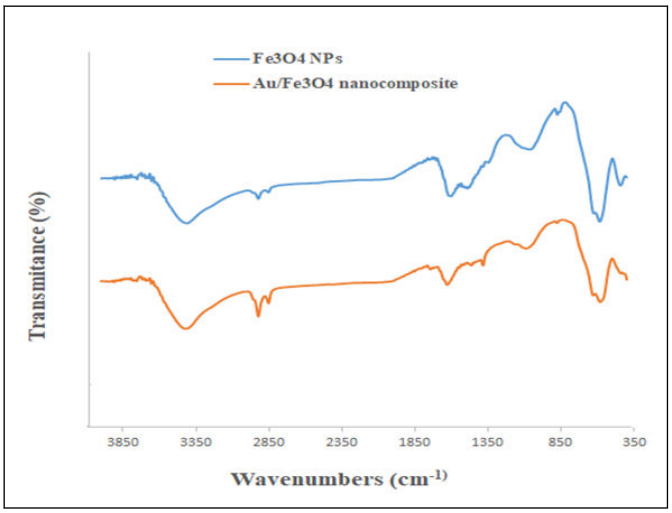


Figure 8: FTIR spectrum obtained from Fe_3O_4 nanoparticle and Au/ Fe_3O_4 nanocomposite.

Based on the results of FE-SEM and determination of the size of Fe_3O_4/Au nanocomposite by ImageJ software, the average particle size for sample 5 is nearly 30 nm with the morphology of spherical, so the particle size dispersions are proper and have a small size difference which is also match able with the results of DLS (Figure 9).

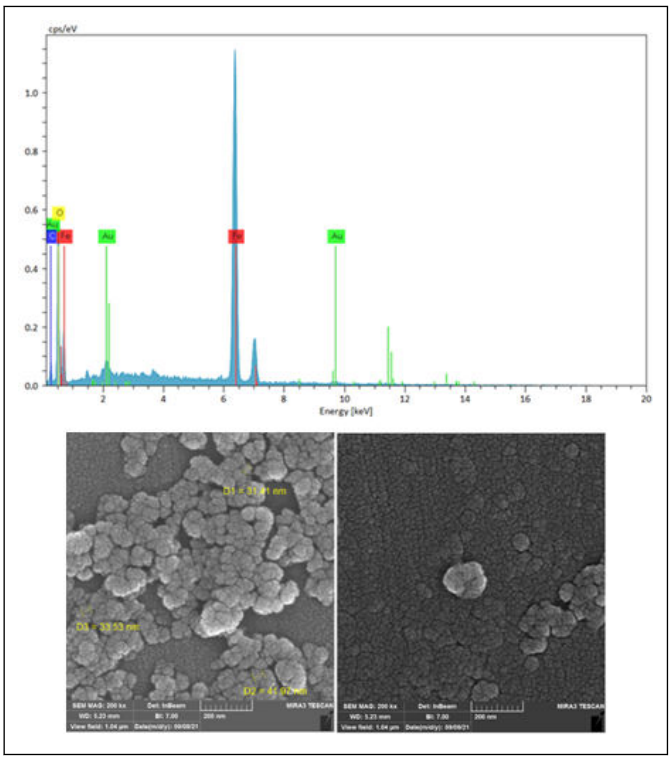
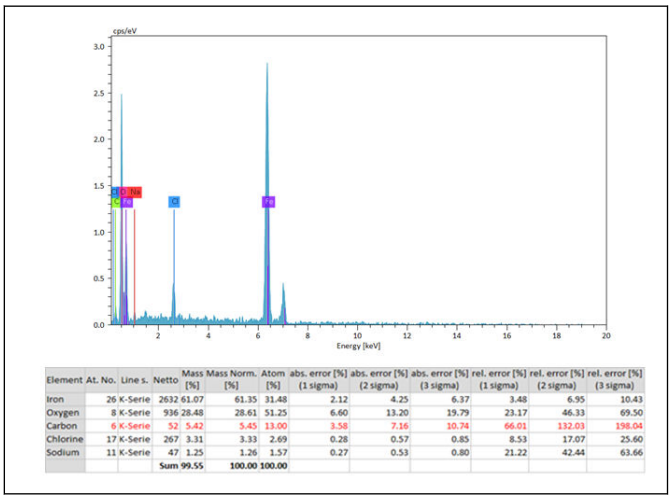


Figure 9: X-ray energy dispersive spectroscopy and FE-SEM images of green synthesized Fe_3O_4/Au NPs (Sample 5).

Energy Dispersive X-ray analysis (EDX) was used to detect and confirm the composition of the synthesized samples that mainly demonstrates the high quantities of Fe and also Au (Figure 4 and Figure 10). Other elements such as carbon due to the coating of NPs with *Malva sylvestris* leave extract are also showed in this analysis.



Element	At. No.	Line s.	Netto	Mass [%]	Mass Norm. [%]	Atom [%]	abs. error [%] (1 sigma)	abs. error [%] (2 sigma)	abs. error [%] (3 sigma)	rel. error [%] (1 sigma)	rel. error [%] (2 sigma)	rel. error [%] (3 sigma)
Iron	26	K-Serie	2632	61.07	61.35	31.48	2.12	4.25	6.37	3.48	6.95	10.43
Oxygen	8	K-Serie	936	28.48	28.61	51.25	6.60	13.20	19.79	23.17	46.33	69.50
Carbon	6	K-Serie	52	5.42	5.45	13.00	3.58	7.16	10.74	66.01	132.03	198.04
Chlorine	17	K-Serie	267	3.31	3.33	2.69	0.28	0.57	0.85	8.53	17.07	25.60
Sodium	11	K-Serie	47	1.25	1.26	1.57	0.27	0.53	0.80	21.22	42.44	63.66
			Sum	99.55	100.00	100.00						

Figure 10: X-ray energy dispersion spectroscopy of Fe_3O_4 nanoparticles.

Conclusion

In summary, we utilized an uncomplicated and green method for the synthesis Fe_3O_4/Au nanoparticle by *Malva sylvestris* leave extract as secure and functional reducing and stabilizing agents. To synthesis of Fe_3O_4/Au nanoplatform using *Malva sylvestris* leave extract with an average size of 30-45 nm and spherical shapes; we optimized some parameters to obtain the nanocomposite with the favorable particle size for using in photothermal therapy method for cancer. The biosynthesized Fe_3O_4/Au NPs were characterized by different techniques. This green approach of synthesizing Fe_3O_4/Au-NPs could also be extended to synthesize other significant metal oxides and nanoparticles for using in photothermal therapy.

Acknowledgements

We thank Kermanshah University of Medical Sciences for financial support of this work.

References

1. Choueiri TK, Motzer RJ (2017) Systemic therapy for metastatic renal-cell carcinoma. N Engl J Med 376: 354–366.
2. Peer D, Karp JM, Hong S, Farokhzad OC, Margalit R, et al. (2007) Nanocarriers as an emerging platform for cancer therapy. Nat Nanotechnol 2: 751–760.
3. Fang RH, Kroll AV, Gao W, Zhang L (2018) Cell membrane coating nanotechnology. Adv Mater 30: e1706759.
4. Wang Z, Liu W, Shi J, Chen N, Fan C (2018) Nanoscale delivery systems for cancer immunotherapy. Mater Horiz 5: 344–362.
5. Ito A, Shinkai M, Honda H, Yoshikawa K, Saga S, et al. (2003) Heat shock protein 70 expression induces antitumor immunity during intracellular hyperthermia using magnetite nanoparticles. Cancer Immunol Immunother 52: 80-88.
6. Lepock JR (2003) Cellular effects of hyperthermia: Relevance to the minimum dose for thermal damage. International Journal of Hyperthermia 19: 252-266.

© Copyright iMedPub

7. He X, Wolkers WF, Crowe JH, Swanlund DJ, Bischof JC (2004) in situ thermal denaturation of proteins in dunning at-1 prostate cancer cells: implication for hyperthermic cell injury. Ann Biomed Eng 32: 1384-1398.

8. Tong L, Cheng JX (2009) Gold nanorod-mediated photothermolysis induces apoptosis of macrophages via damage of mitochondria. Nanomedicine (Lond) 4: 265-276.

9. Mocan T, Matea CT, Cojocaru I, Ilie I, Tabaran FA, et al. (2014) Photothermal Treatment of Human Pancreatic Cancer Using PEGylated Multi-Walled Carbon Nanotubes Induces Apoptosis by Triggering Mitochondrial Membrane Depolarization Mechanism. Cancer J 5: 679-88.

10. Hirsch LR, Stafford RJ, Bankson JA, Sershen SR, Rivera B, et al. (2003) nanoshell mediated near-infrared thermal therapy of tumors under magnetic resonance guidance. Proc Natl Acad Sci USA 100: 13549-13554.

11. Hildebrandt B, Wust P, Ahlers O, Dieing A, Sreenivasa G, et al. (2002) The cellular and molecular basis of hyperthermia. Crit Rev Oncol Hematol 43: 33-56.

12. Melamed JR, Edelstein RS, Day ES (2015) Elucidating the Fundamental Mechanisms of Cell Death Triggered by Photothermal Therapy. ACS Nano 9: 6-11.

13. Gobin AM, Lee MH, Halas NJ, James WD, Drezek RA, et al. (2007) Near-infrared resonant nanoshells for combined optical imaging and photothermal cancer therapy. Nano letters 7: 1929-1934.

14. Weissleder R (2001) A clearer vision for in vivo imaging. Nat Biotechnol 19: 316-317.

15. Vogel A, Venugopalan V (2003) Mechanisms of Pulsed Laser Ablation of Biological Tissues. Chem Rev 103: 577-644.

16. Wang Y, Black KC, Luehmann H, Li W, Zhang Y, et al. (2013) Comparison Study of Gold Nanohexapods, Nanorods, and Nanocages for Photothermal Cancer Treatment. ACS Nano 7: 2068-2077.

17. Moon HK, Lee SH, Choi HC (2009) In vivo Near-Infrared Mediated Tumor Destruction By Photothermal Effect Of Carbon Nanotubes. ACS Nano 3: 3707-3713.

18. Manikandan M, Hasan N, Wu HF (2013) Platinum nanoparticles for the photothermal treatment of Neuro 2A cancer cells. Biomaterials 34: 5833-5842.

19. Li Y, Lu W, Huang Q, Huang M, Li C, et al. (2010) Copper sulfide nanoparticles for photothermal ablation of tumor cells. Nanomedicine (Lond) 5: 1161-1171.

20. Yang J, Choi J, Bang D, Kim E, Lim EK, et al. (2011) Convertible organic nanoparticles for near-infrared photothermal ablation of cancer cells. Angew Chem Int Ed 50: 441–444.

21. Pitsillides CM, Joe EK, Wei X, Anderson RR, Lin CP (2003) Selective cell targeting with light absorbing microparticles and nanoparticles. Biophys J 84: 4023–32.

22. Vankayala R, Lin CC, Kalluru P, Chiang CS, Hwang KC (2014) Gold nanoshells-mediated bimodal photodynamic and photothermal cancer treatment using ultra-low doses of near infra-red light. Biomaterials 35: 5527-38.

23. Jang B, Park JY, Tung CH, Kim IH, Choi Y (2011) Gold Nanorod −Photosensitizer Complex for Near-Infrared Fluorescence Imaging and Photodynamic/Photothermal Therapy In Vivo. ACS Nano 5: 1086-1094.

24. Li C, Chen T, Ocsoy I, Zhu G, Yasun E, et al. (2014) Gold-Coated Fe3O4 Nanoroses with Five Unique Functions for Cancer Cell Targeting, Imaging, and Therapy. Adv Funct Mater 24: 1772-1780.

25. Ismail E, Sabry D, Mahdy H, Khalil M (2014) Synthesis and Characterization of some Ternary Metal Complexes of Curcumin with 1,10-phenanthroline and their Anticancer Applications. J Sci Res 6: 509-519.

26. Rajeshkumar S (2016) Anticancer activity of eco-friendly gold nanoparticles against lung and liver cancer cells. J Genet Eng Biotechnol 14: 195-202.

27. Niranjan Dhanasekar N, Ravindran Rahul G, Badri Narayanan K, Raman G, Sakthivel N (2015) Green chemistry approach for the synthesis of gold nanoparticles using the fungus Alternaria sp. J Microbiol Biotechnol 25: 1129-1135.